

LASERS

https://doi.org/10.1070/QEL16533

Highly efficient red single transverse mode superluminescent diodes

E.V. Andreeva, A.S. Anikeev, S.N. Il'chenko, A.Yu. Chamorovskii, S.D. Yakubovich

Abstract. **Optimisation of the epitaxial growth of AlGaInP/GaInPAs nanoheterostructures and improvement of the technologies of active channel formation and p-contact deposition made it possible to considerably increase the external differential quantum efficiency (up to 0.5 mW mA^{-1}), the catastrophic optical degradation threshold (up to 40 mW), and the spectral width (to FWHM exceeding 15 nm) of single transverse mode superluminescent diodes with the centre wavelength of about 675 nm. Lifetime tests demonstrated high reliability of these diodes at a cw output optical power up to 30 mW.**

Keywords: *semiconductor multiquantum well, superluminescent diode, red spectral range.*

1. Introduction

Red semiconductor red laser diodes (LDs) based on AlGaInP/GaInPAs heterostructures have found the widest application. They are used in optical schemes of information writing and reading, in medical devices, laser pointers, rangefinders, laser sights, and a number of other devices. Estimates of Strategies Unlimited (USA) show that the annual output of these lasers is hundreds of millions. Hundreds of publications are devoted to their investigation and improvement. At the same time, production of red superluminescent diodes (SLDs), which were developed more than 20 years ago [1], is several orders of magnitude lower and, according to our estimates, is several thousands of diodes per year. Publications devoted to these diodes can be counted on fingers. However, red SLDs turned out to be optimal light sources for some practical applications (atomic-force microscopy [2], low-coherence illumination [3,4], medico-biological studies and therapy [5–8]).

The achievable output optical power of red laser diodes is close to that of near-IR LDs based on AlGaAs/InGaAs heterostructures (hundreds of milliwatts for cw single transverse mode diodes with the active channel width of several micrometres). For both diode types, the output power is restricted by the threshold of catastrophic optical damage (COD) related, as a rule, to destruction of end mirrors. The optical output power level of red SLDs is an order of magnitude lower. The output power of commercial diodes emitting in the spectral range 650–680 nm (SUPERLUM, EXALOS, NoLaTech, Inject, QPhotonics) does not exceed 15 mW (SLD-26-HP, SUPERLUM) [9,10]. As a rule, COD, which restricts this power, is not related to destruction of faces. As is known, SLDs differ from LDs by a considerably higher concentration of nonequilibrium charge carriers in the working regime. Nevertheless, the output power of most efficient SLDs in the violet-blue and near-IR spectral ranges approaches, in the order of magnitude, the power of LDs with the same sizes of the active channel (see, e.g., [11,12]). We do not known works aimed at revealing the key degradation mechanism of red SLDs.

In the present work, we study SLDs with the centre wavelength of about 675 nm fabricated by improved technologies of epitaxial growth of nanoheterostructures, active channel formation, and p-contact deposition. The output characteristics of these SLDs are much better than those of commercial analogues.

2. Experimental samples

Over the years, the aforementioned SLD-26-HP diodes are fabricated based on a triple quantum-well heterostructure [9] grown on a GaAs substrate oriented in the (100) crystallographic plane. In the present work, we in general reproduced this heterostructure on a substrate disoriented by an angle of 6° with respect to one of the cleavage planes using MOCVD equipment with a horizontal AIXTRON AIX 200/4 reactor. In addition, we improved the technology of formation of single-mode ridge waveguides, which ensured a stronger lateral optical confinement and a weaker optical limiting in the direction perpendicular to the heterolayers of the 'new' heterostructure compared to the conventional ('old') heterostructure (Fig. 1). Looking ahead, we should note that this led to a rather high (60%–70%) coefficient of coupling the SLD radiation into single-mode fibres with the use of a cylindrical end microlens. Previously, this coefficient did not exceed 55%. The high homogeneity of the grown heterostructure and the high quality of its post-growth processing is evidenced by the histogram in Fig. 2, which illustrates the reproducibility of the centre superluminescence wavelength of samples with identical configurations fabricated from different regions of conventionally used ('old') and the optimised ('new') heterostructures.

The developed complex of photolithographic masks made it possible to fabricate active SLD channels with the width $w = 2$ and 4 μm. Their axes formed an angle of 7° with respect to the normal to the cleavage plane of the crystal. The active

E.V. Andreeva, A.S. Anikeev, S.N. Il'chenko Opton LLC, ul. Mosfil'movskaya 17b, 119330 Moscow, Russia;
A.Yu. Chamorovskii Superlum Ltd., Unit B3, Fota Point Enterprise Park, Carrightwohill, Co Cork, Ireland;
S.D. Yakubovich Moscow Technological University (MIREA), prosp. Vernadskogo 78, 119454 Moscow, Russia;
e-mail: yakubovich@superlumdiodes.com

Received 11 October 2017
Kvantovaya Elektronika **47** (12) 1154–1157 (2017)
Translated by M.N. Basieva

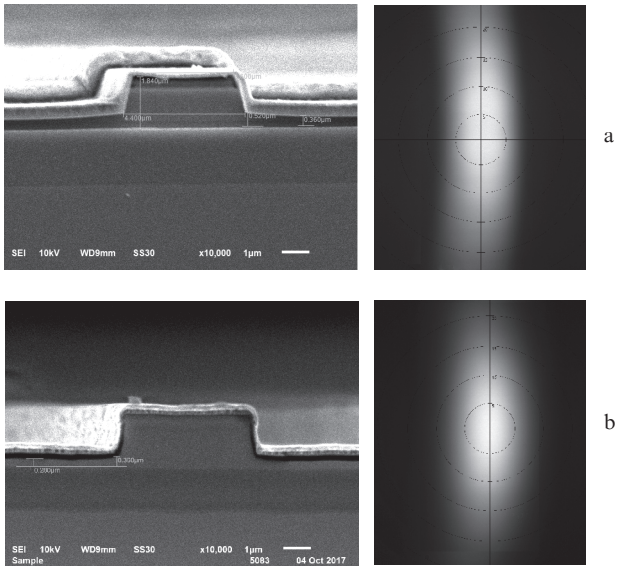

Figure 1. Microphotographs of the active channels ends (w = 4 μm) and the cross sections of output beams of (a) 'old' and (b) 'new' SLDs.

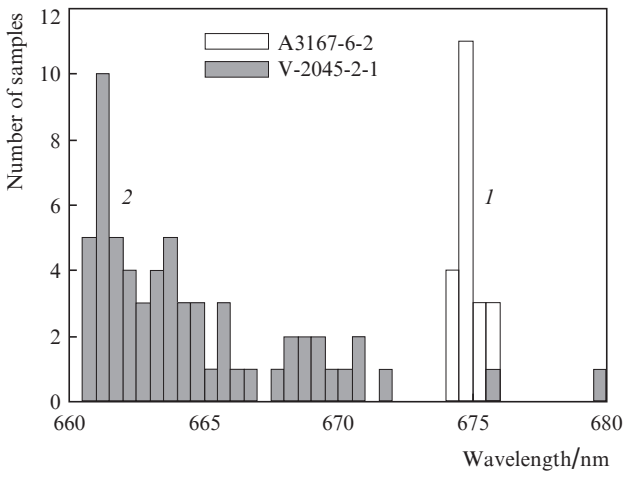

Figure 2. Histogram illustrating reproducibility of the median wavelength of (*1*) 'new' and (*2*) 'old' SLDs of identical configurations under identical operating conditions.

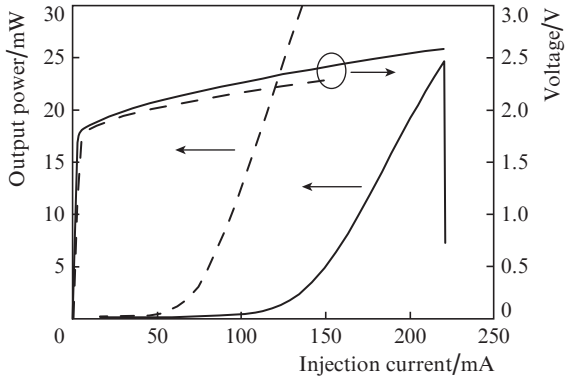

Figure 3. Current–voltage and power–current characteristics of (solid corves) 'old' and (dashed curves) 'new' SLDs of identical configurations (L_a = 1200 μm, w = 4 μm).

channel length L_a was determined by the cleavage points and varied from 200 to 2000 μm. The crystal faces were coated by two antireflection layers. Figure 3 shows typical current–voltage and power–current characteristics of the best 'old' and 'new' SLDs of identical configurations (w = 4 μm, L_a = 1200 μm). The presented curves clearly demonstrate considerable superiority of the developed samples in differential resistance, external quantum efficiency, and COD threshold.

3. Main physical characteristics of studied SLDs

Figure 4 shows typical power–current characteristics of SLD samples with w = 4 μm and different L_a upon continuous injection at a temperature of 25°C. At small L_a (no larger than 800 μm), the output optical power is limited by thermal saturation. At large L_a, this limit is determined by the COD threshold, which is 35–40 mW and is almost independent of L_a. Thus, this COD threshold value is determined mainly by the light flux density at the SLD output. From this it follows that it is useless to make SLDs with L_a exceeding 1200–1400 μm in order to increase the output power. It should be noted that the aforementioned COD threshold values were recorded for long SLDs after operation for 120–150 h. The COD threshold of about 50 mW reported in [13] was recorded for freshly prepared samples.

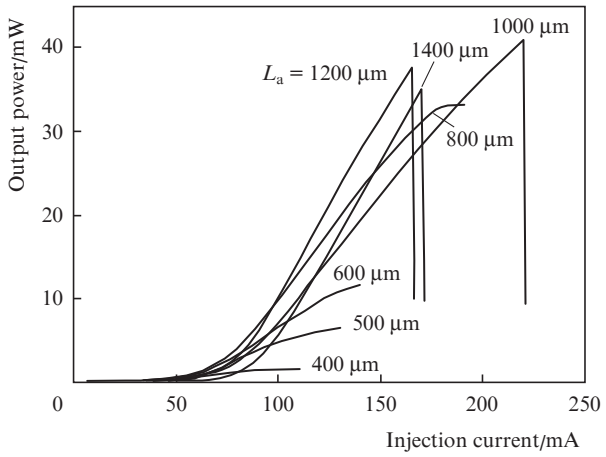

Figure 4. Typical power–current characteristics of SLDs with different active channel lengths (w = 4 μm).

The radiation of all the samples in the developed superluminescence regime was strongly polarised, with the TE/TM ratio exceeding 20 dB. The depth of residual Fabry–Perot spectral modulation did not exceed 2%.

The samples of SLDs with w = 2 μm have a higher differential quantum efficiency, but their COD threshold is 20–25 mW. Their fabrication is reasonable if the required output power does not exceed 15 mW.

Table 1 presents typical output parameters of the studied SLD samples. It is important to note that SLDs with short L_a at an output power of several mW may have output spectra with a FWHM up to 20 nm (with a coherence length shorter than 10 μm), while the spectral halfwidth of commercial red SLDs does not exceed 10 nm. For some practical applications of SLDs, for example, for optical coherence tomography, this parameter is crucial.

Table 1. Main parameters of SLDs with different active channel dimensions.

w/ μm	L_a/ μm	I/ mA	J/ kA cm^{-2}	P_{FS}/ mW	P_{SM}/ mW	λ_m/ nm	$\Delta\lambda$/ nm	MTTF/ h
	400	80	1.05	2.0	0.9	675	19.0	2 500
	500	110	1.09	6.0	3.3	674	14.0	5 000
2.0	600	110	0.91	11.5	6.9	674	12.1	10 000
	1000	110	0.57	16.0	11.2	670	8.6	n/a
	1200	110	0.46	18.4	12.9	673	7.5	20 000
	400	90	0.56	1.8	0.7	675	19.5	20 000
	500	120	0.59	7.1	3.6	673	14.9	20 000
	600	150	0.58	12.2	8.2	673	12.6	25 000
4.0	800	150	0.44	21.9	15.1	670	9.6	n/a
	1000	150	0.35	23.0	16.1	672	8.8	n/a
	1200	150	0.29	31.5	22.0	674	8.2	30 000
	1400	150	0.25	25.3	17.7	677	7.1	35 000

Note: w is the ridge waveguide width; L_a is the active channel length; I is the injection current; J is the injection current density; P_{FS} is the free space output power; P_{SM} is the output power through the SMF; λ_m is the median wavelength; $\Delta\lambda$ is the spectral halfwidth and MTTF is the mean time to failure at 25°C.

Figure 5 shows the typical spectra of SLDs with L_a equal to 500 and 1400 μm and the corresponding coherence functions (CFs). The spectral shape is close to Gaussian, because of which the central CF peak has no pedestal typical for spectra with other profiles. These CFs are optimal for light sources used in interferometers because they ensure the maximum sensitivity. Of undoubted interest is the use of developed SLDs as active elements of semiconductor optical amplifiers (SOAs), which can serve as a basis for development of lasers tunable within the range 665–685 nm, as described in [14].

Figure 6 shows the dependences of the median wavelength and the spectral linewidth of the same SLD samples on the injection current at a fixed temperature of the SLD submount and on temperature at a fixed injection current. This figure also presents the temperature dependences of the output power. The given curves show that the spectral parameters of long high-power SLDs at a stabilised temperature only slightly depend on the injection current, while the wavelength and spectral halfwidth of short broadband SLDs noticeably increase with increasing current, which is related to a higher thermal resistance of the latter diodes. Thus, long SLDS can be used in the automatic power control regime, while stabilisation of injection current is preferable for short SLDs.

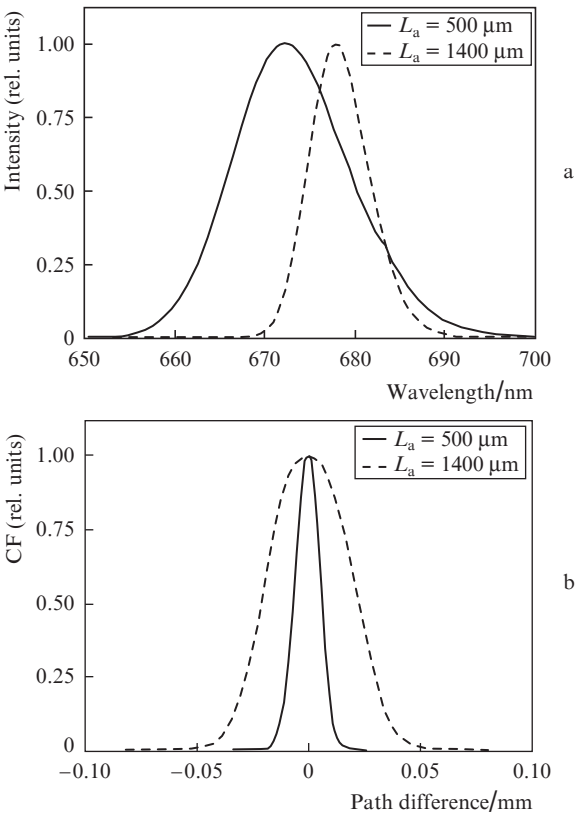

Figure 5. (a) Spectra and (b) CFs of SLDs (w = 4 μm) with L_a = 500 and 1400 μm.

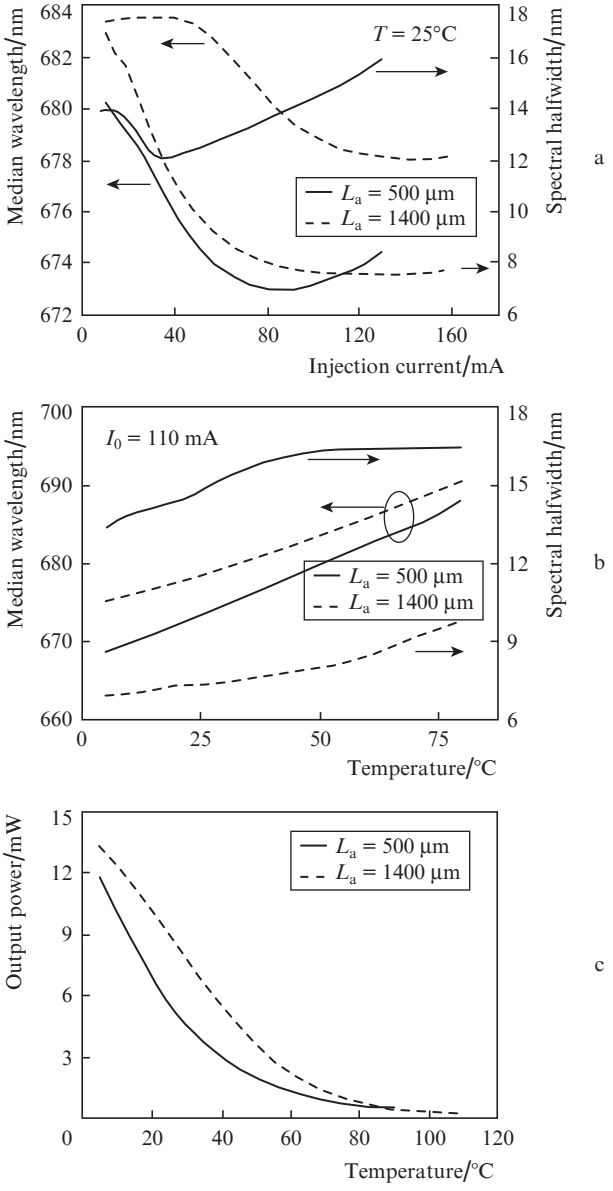

Figure 6. Dependences of the median wavelength λ_m and the spectral halfwidth $\Delta\lambda$ (a) on the injection current at T = 25°C and (b) on temperature at current I = 110 mA for the same samples as in Fig. 5, as well as (c) temperature dependences of their output power.

Figures 6b and 6c illustrate a strong temperature dependence of the output power and spectral characteristics of the studied SLDs and indicate that thermostabilisation in necessary for most practical applications.

Figure 7 presents the chronograms of preliminary lifetime tests in the regime of automatic current control at $T = 25$°C for SLDs with lengths of 500 and 1400 μm. The mean time to failure (MTTF) was estimated by the conventional method, i. e., by linear extrapolation of the curves to a 50% decrease in the output power. The obtained MTTF values are listed in the rightmost column of Table 1. The service lifetime for most practical applications of SLDs exceeds 20000 h and is acceptable. It should be noted that fabrication of broadband SLDs with $w = 2$ μm is inexpedient due to their relatively low reliability.

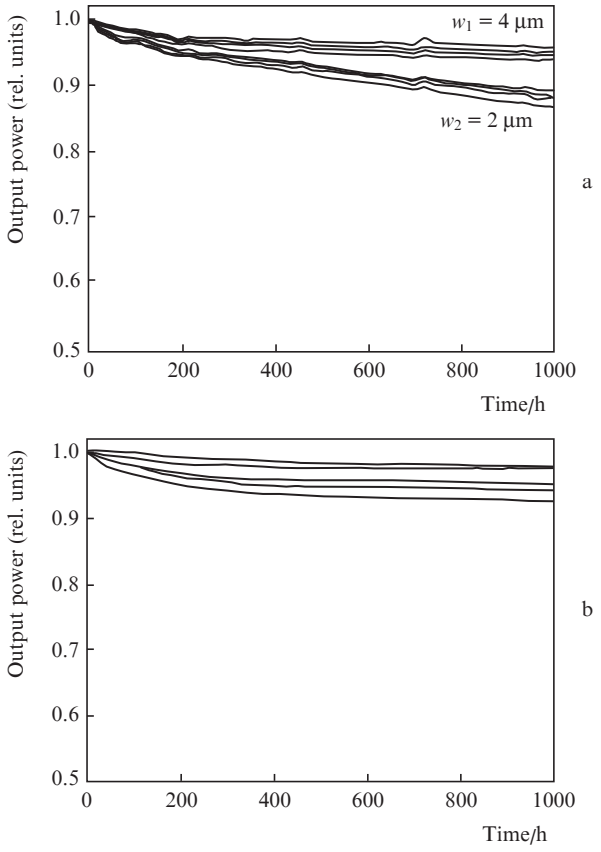

Figure 7. Chronograms of preliminary lifetime tests of SLDs with active channel lengths L_a = (a) 500 μm ($w_1 = 2$ μm, $I_1 = 110$ mA; $w_2 = 4$ μm, $I_2 = 120$ mA) and (b) 1400 μm ($w = 4$ μm, $I = 150$ mA).

At present, SLDs of the new series SLD-26-UHP (P_{FS} = 25 mW, P_{SM} = 15 mW) are being introduced into industry.

Thus, the improvement of the growth and post-growth technologies of AlGaInP/GaInPAs triple quantum wells made it possible to develop rather reliable red SLDs of conventional configuration, whose main characteristics are one and half to two times higher than those of commercial diodes of this type.

Acknowledgements. The authors are grateful to V.R. Shidlovskii for the initiation of this study. The work was partially supported by the Ministry of Education and Science of the Russian Federation (Project No. 8.4853.2017/BCh).

References

1. Semenov A.T., Shidlovski V.R., Safin S.A., Konyaev V.P., Zverkov M.V. *Electron. Lett.*, **29** (6), 530 (1993).
2. Rode S., Stark R., Lübbe J., Tröger L., Schütte J., Umeda K., Kobayashi K., Yamada H., Kühnle A. *Rev. Sci. Instrum.*, **82** (073703), 073703-1 (2011).
3. Gastinger K., Løvhaugen P., Skotheim Ø., Hunderi O. *Proc. SPIE*, **6616**, 66163K-1 (2007).
4. Lansdorp B.M., Tabrizi S.J., Dittmore A., Saleh O.A. *Rev. Sci. Instrum.*, **84** (044301), 044301-1 (2013).
5. Storen T., Simonsen A., Royset A.K., Lokberg O.J., Svaasand L.O., Tore Lindmo T. *Proc. SPIE*, **4956**, 197 (2003).
6. Li H., Lu J., Shi G., Zhang Y. *J. Biomed. Opt.*, **16** (11), 110504 (2011).
7. Zawadzki R., Zhang P., Zam A., Miller E., Goswami M., Wang X., Jonnal R., Lee S., Kim D., Flannery J., Werner J., Burns M., Pugh E. *Biomed. Opt. Express*, **6**, 2191 (2015).
8. Karu T., Andreichuk T., Ryabykh T. *Lasers Surg. Med.*, **13** (4), 453 (1993).
9. Ryaboshtan Yu.L., Gorlachuk P.V., Marmalyuk A.A., Lobintsov A.A., Il'chenko S.N., Yakubovich S.D. *Trudy XVI Mezhdun. simp. 'Nanofizika i nanoelektronika'*, **2**, 372 (2012).
10. Padalitsa A., Marmalyuk A., Yarotskaya I., Gorlachuk P., Ryaboshtan Yu., Il'chenko S., Lobintsov A., Yakubovich S. *17th Int. Conf. MOVPE* (Lausanne, 2014) Web-Poster 0-71, p. 1.
11. Andreeva E.V., Il'chenko S.N., Kurnyavko Yu.V., Luk'yanov V.N., Shidlovskii V.R., Yakubovich S.D. *Quantum Electron.*, **46** (7), 594 (2016) [*Kvantovaya Elektron.*, **46** (7), 594 (2016)].
12. Kefar A., Standzic S., Wisnievski P., Oto T., Makarova I., Targovski G., Suski T., Perlin P. *Phys. Stat. Solidi A*, **212** (5), 997 (2015).
13. Andreeva E.V., Anikeev A.S., Il'chenko S.N., Chamorovsky A.Yu., Yakubovich S.D. *Electron. Lett.*, **53** (23), 1539 (2017).
14. Kostin Yu.O., Ladugin M.A., Lobintsov A.A., Marmalyuk A.A., Chamorovskii A.Yu., Shramenko M.V., Yakubovich S.D. *Quantum Electron.*, **45** (8), 697 (2015) [*Kvantovaya Elektron.*, **45** (8), 697 (2015)].